Applied Physics A (2022) 128:467
https://doi.org/10.1007/s00339-022-05621-x

Applied Physics A
Materials Science & Processing

Hexa-sectored square photonic crystal fiber for blood serum and plasma sensing with ultralow confinement loss

Sayed Asaduzzaman[1,3] · Hasin Rehana[2,3] · Rana Chakma[1] · Osama S. Faragallah[4] · Hala S. El-Sayed[5] · Mahmoud M. A. Eid[6] · Ahmed Nabih Zaki Rashed[7]

Received: 6 January 2022 / Accepted: 19 April 2022 / Published online: 6 May 2022

Abstract

This study suggested a novel hexa-sectored square photonic crystal fiber (HS-SPCF) for blood serum and blood plasma sensing. The proposed HS-SPCF depicts an eminent sensitivity of blood plasma 66.7% and blood serum73.4% with ultralow low confinement loss 1.55×10^{-12} and 10.55×10^{-12} at the wavelength of 1.33 µm for blood plasma and serum. The operating wavelength to measure the optical properties using FEM was 0.6–1.6 µm. The proposed HS-SPCF showed ameliorating performance in confinement loss and relative sensitivity than the previous structures for blood components sensing. In addition, other optical characteristics like high birefringence of 2.6×10^{-3} and 2.6×10^{-3}, lower EML of 0.21247 (cm^{-1}) and 0.2170 (cm^{-1}), effective area of 6.1 μm^2 and 6.4 μm^2, nonlinearity of 21.1(W^{-1} km^{-1}) and 19.6 (W^{-1} km^{-1}), numerical aperture (NA) of 0.286 and 0.281 has been achieved for proposed PCF at the wavelength of 1.33 µm. The proposed PCF will be used for biosensing or blood-sensing purposes and a broad diversity of chemical sensing functions.

Keywords HS-SPCF · Blood sensor · Serum sensor · Plasma sensor · Confinement loss · Relative sensitivity

1 Introduction

Throughout recent years, photonic crystal fibers (PCFs) diversifies the application of sensors among researchers for their flexible structural characteristics, abundant model features, light-guiding properties, etc. [1, 2]. Comparing to conventional optical fibers Photonic crystal fibers exhibits better performance in term of high relative sensitivity, lower confinement loss, PCF are being used during the recent years as stress sensors [3], temperature sensors [4], chemical sensors [5], biosensors [6], pH sensors [7] with different structures. Refractive Index (RI) based sensor has now been

✉ Ahmed Nabih Zaki Rashed
ahmed_733@yahoo.com

Sayed Asaduzzaman
s.asaduzzaman.bd@ieee.org

Hasin Rehana
hasin.cse13@gmail.com

Rana Chakma
ranachakma@gmail.com

Osama S. Faragallah
o.salah@tu.edu.sa

Hala S. El-Sayed
hall_hhh@yahoo.com

Mahmoud M. A. Eid
m.elfateh@tu.edu.sa

[1] Department of Computer Science and Engineering, Rangamati Science and Technology University, Rangamati, Bangladesh

[2] Department of Computer Science and Engineering, University of Dhaka, Dhaka, Bangladesh

[3] Department of Computer Science and Engineering, Daffodil International University, Dhaka, Bangladesh

[4] Department of Information Technology, College of Computers and Information Technology, Taif University, P.O. Box 11099, Taif 21944, Saudi Arabia

[5] Department of Electrical Engineering, Faculty of Engineering, Menoufia University, Shebin El-Kom 32511, Egypt

[6] Department of Electrical Engineering, College of Engineering, Taif University, P.O. Box 11099, Taif 21944, Saudi Arabia

[7] Department of Electronics and Electrical Communications Engineering, Faculty of Electronic Engineering, Menoufia University, Menouf 32951, Egypt

widely used in biological liquid sensing. RI-based sensors mainly work by selectively filling the air hole at the core region where the light interacts with the liquid analytes filled in the micron area of the PCF. There are two types of RI sensor techniques. They are—internal and external sensing techniques [8]. Various types of Photonic Crystal Fiber have been proposed past few years for sensing applications. S. Asaduzzaman et al. proposed a gas sensor where cladding regions were hexagonal shaped with a slotted core [9]. In [10], rhombic core-based hexagonal H-PCF has been suggested for chemical detection purposes where both elliptical and circular holes have been used. A chemical ($n = 1.354$) has been detected by relative sensitivity where the core rhombic region was filled with the chemical which interacts with light. In 2016 M. I Islam et al. proposed a unique spiral-shaped PCF for gas sensing application, demonstrating higher relative sensitivity than the previous Structures [11]. The core region of the proposed structure was arranged with elliptical-shaped holes in a hexagonal formation. Alcohol (methanol, ethanol, propanol, butanol, pentanol) sensors were designed in [12]. In the proposed sensor, the cladding region was octagonal, and the core region was varied with 2,3 and 4 layers of circular holes in a circular formation.

For derivative total internal reflection techniques to compute distribution in a sample [13], transmission electron microscopy [14], and optical coherent tomography [15], the optical attributes of blood components are much needed. The significant divergence between blood plasma and serum is the presence of fibrinogen. In clinical analysis, Blood plasma and serum both are substantial biochemical samples [16]. In [17], by the total internal reflection technique, the refractive index of various types of human blood was detected. These values of refractive index impact pathology and diagnosis in medical science. For the monitoring of diabetes mellitus, the glycation process and determining glycated proteins are very significant. Change of Refractive Index of albumin and hemoglobin and association with glucose is a potential technique for examining the glycated proteins and glycation action [18].

The main and scope of this research are (i) design and analyze a novel photonic crystal fiber structure. (ii) To detect blood components with high relative sensitivity. (iii) To gain better optical properties like relative sensitivity, confinement loss, effective material loss, numerical aperture, nonlinearity. (iv) To analyze the optical properties at a wider range of operating wavelength. (v) To optimize the designing parameters of PCF which can be used for practical purpose. (vi) To compare the proposed PCF with prior PCFs.

In this article, a square shape hybrid cladding PCF has been proposed with the hexa-sectored core region. The core region was filled with blood plasma and serum as blood components which expresses higher relative sensitivity than the previous research [16, 17]. The real part of the blood serum and plasma was achieved from Cauchy's equation from a wide range of wavelengths. The proposed PCF shows ultralow confinement loss and shows good results in birefringence, NA, EML, Effective area, and nonlinearity. The whole work has been described by Design and Numerical Analysis, Results and Discussion, and Conclusion sections step by step.

2 Design methodology and numerical investigation

Figure 1a depicts the cross-sectional perspective of the proposed hexa-sectored square shaped PCF (HS-SPCF). The core area of the following PCF is hexagonal shaped sectored into six triangular regions. The hexa-shaped PCF contains a square solid sectored area at the center. Hexa-sectored core has a diameter denoted by $D = 1.6$ µm. The cladding region is a hybrid structure with circular holes and square holes. The diameter of the circular holes is denoted by $d_2 = (0.95 \times \Lambda_2)$ arranged in a square shape with four adjacent layers. The diameter of the square holes is denoted by $d_1 = 0.6$ µm and arranged in a square arrangement. Also, the center to center distance of two adjacent holes is called pitch. Here, the square hole pitch is denoted by $\Lambda_1 = 0.8$ µm and $\Lambda_2 = 0.8$ µm denotes the pitch of the circular holes.

To design the proposed HS-PCF, we have considered some background information on photonic crystal fiber. In [19], authors have proposed s square shape cladding based PCF, which shows better optical properties like birefringence, nonlinearity, etc. Hybrid structure photonic crystal fiber has drawn the attraction of researchers as it shows better optical properties [9, 10, 20]. Share hole or slotted rectangular type hole is very effective in sensing purposes shown in [9]. So considering all the properties, we have designed a novel structure hybrid HS-PCF. The core region is kept hexagonal sectored, which can hold blood components at the core region.

Figure 1b shows the experimental setup for the proposed HS- PCF. The core region of the proposed PCF is filled with blood components (blood serum/blood plasma). There is a big question that the core region is consists of a square solid hole surrounded with hexagonal shaped six triangular regions. So, if all of those will fill with blood serum/blood plasma, why instead of using single hexagonal shaped hole with same D, six peace of triangular and solid square are used? This is because core square solid region will be used to make integrity of the adjacent six holes. As there may be one hole instead of six hole. If we made one hole and fill blood serum or plasma it may cause the collapse the holes with other holes. A spectrograph device is also used in this experimental setup. Fiber lasers pass light through the proposed PCF, and due to

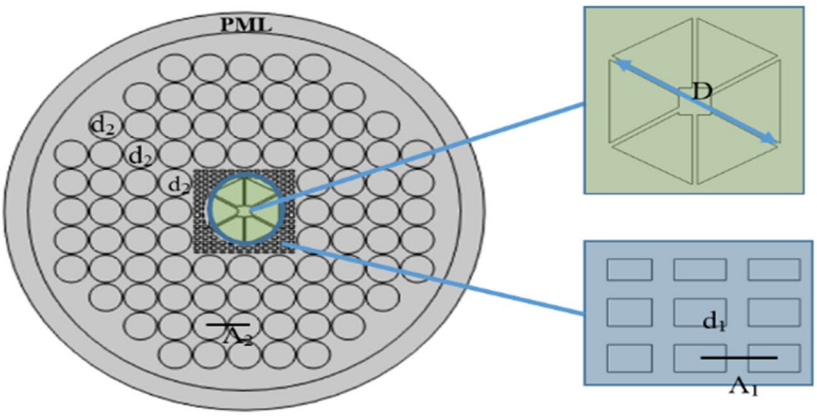

(a) The proposed HS-SPCF (Cross-Section).

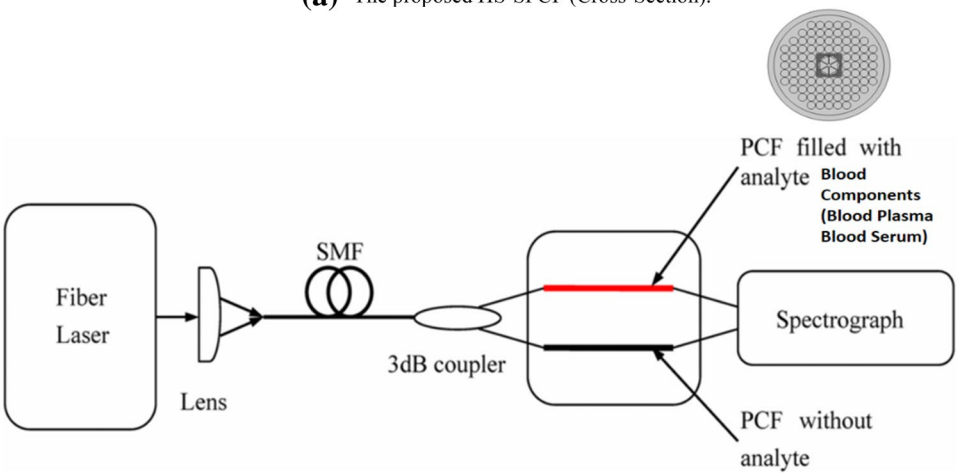

(b) Experimental Setup for Proposed PCF as a Sensor.

Fig. 1 **a** The proposed HS-SPCF (Cross-Section). **b** experimental setup for proposed PCF as a sensor

the higher refractive index of the core (as it is filled with Blood serum and plasma), the fundamental mode will be at the core. The background material was kept silica, and PML (Perfectly Matched Layer) was kept 10% higher than the total fiber diameter.

The $n(\lambda) = \sqrt{1 + \frac{A_1\lambda^2}{\lambda^2 - C_1} + \frac{A_2\lambda^2}{\lambda^2 - C_2} + \frac{A_3\lambda^2}{\lambda^2 - C_3}}$ Refractive index of silica has been achieved by the Sellmeier equation [20]

$$n(\lambda) = \sqrt{1 + \frac{A_1\lambda^2}{\lambda^2 - C_1} + \frac{A_2\lambda^2}{\lambda^2 - C_2} + \frac{A_3\lambda^2}{\lambda^2 - C_3}} \quad (1)$$

Here in this research, we have sensed blood serum and blood plasma. The characteristics of both blood serum and blood plasma is that the RI (refractive index) of both blood constituents decreases with the increase of wavelength [21]. Therefore, we have used the Cauchy's equation [21] to evaluate blood serum and blood plasma refractive index. Here in the Eq. (1) and (2) λ is the operating wavelength. A_1, A_2, A_3, C_1, C_2, C_3 in Eq. (1) are constant values.

$$n_r = A + \frac{B}{\lambda^2} + \frac{C}{\lambda^4} \quad (2)$$

where A, B, and C are Cauchy's coefficients has been shown in Table 1 [22].

Relative sensitivity is the most important optical characteristic that illustrates photonic crystal fiber as a sensor. The relative sensitivity can be obtained by Eq. 3 and Eq. 4 [23]. The higher the relative sensitivity (RS), the better the sensor. Here in Eq. 3, n_r and n_{eff} are the refractive index of analytes (Plasma/Serum) and effective refractive index of the proposed Photonic Crystal Fiber. P is the power fraction of the power of the sample power at the core and total power. E_x and E are the

Table 1 Blood serum, blood plasma Cauchy's coefficients

Analyte sample	Blood serum	Blood plasma
A	1.3350	1.3353
B	4.6513×10^3	4.4048×10^3
C	-1.3069×10^8	-9.1925×10^7

electric fields according to the x and y-axis, and H_x and H_y are the magnetic fields according to the x and y-axis.

$$r = \frac{n_r}{n_{eff}} \times p\% \tag{3}$$

$$p = \frac{\int\limits_{sample} R_e(E_x H_y - E_y H_x)dxdy}{\int\limits_{total} R_e(E_x H_y - E_y H_x)dxdy} \times 100 \tag{4}$$

Another important parameter is confinement loss (CL) due to the scattering of light through the cladding region at the transmission of light [24]. Confinement loss can be calculated by Eq. 5, where Im (n_{eff}) is the imaginary part of the effective refractive index. Effective Material Loss can be calculated by Eq. 6, which defines from the light source minimum needed incident light energy [24].

$$CL = 8.686 \times \frac{2\pi f}{c} \mathrm{Im}(n_{eff}) \tag{5}$$

$$EML = \frac{(\varepsilon_0/\mu_0)^{1/2} \int\limits_{A_{mat}} n\alpha_{mat}|E|^2 dA}{2\int\limits_{All} S_Z dA} \tag{6}$$

Effective area (A_{eff}) and nonlinearity (γ) are two significant related characteristics of PCF that can be estimated mathematically by Eq. 7 and Eq. 8. Here in Eq. 7, r is the core radius, and I(r) is the fiber cross-sectional electric field density [24]. For PCF based optical waveguide, numerical aperture is a significant parameter. For PCF based sensors, NA should be higher. NA can be calculated by Eq. 9. A_{eff} is the effective area of the proposed PCF fiber and n_{eff} is the effective refractive index.

$$A_{eff} = \frac{[\int I(r)rdr]^2}{[\int I^2(r)dr]^2} \tag{7}$$

$$\gamma = (\frac{2\pi}{\lambda})(\frac{n_2}{A_{eff}}) \tag{8}$$

$$NA = \frac{1}{\sqrt{1 + \frac{\pi A_{eff} f^2}{c^2}}} \tag{9}$$

The difference between modal effective index along x-polarization and y-polarization is addressed as Birefringence B, computed by Eq. 10 [19].

$$B = \left|n_x - n_y\right| \tag{10}$$

3 Results and discussion

The proposed structure has been designed and numerically analyzed in simulation software COMSOL Multiphysics Version 5. Background material was used as silica, where the Sellmeier equation was used to detect the refractive index. The PCF structure is designed in COMSOL into the 2-D plane. All the numerical equations were set in the simulation software COMSOL and numerically appropriately investigated. The fundamental mode of the suggested HS-SPCF fiber has been expressed in Figs. 2a, b for blood plasma and Fig. 2c, d for blood serum. All the fundamental mode is uniformly distributed along the core region as light-matter interaction occurs with analytes (blood serum/blood plasma). The fundamental mode was captured at the x-axis and y-axis at effective refractive index 1.3496 and 1.3499 for Blood Plasma and effective refractive index 1.3561 and 1.3564 for Blood serum consecutively.

Figure 3 shows the relative sensitivity curve for blood plasma and blood serum. The curve for both blood components increases sharply with respect to wavelength. From 0.6 to 1 µm, the curve for plasma and serum are almost the same, but after that, the relative sensitivity curve increases a bit higher than blood plasma. The highest sensitivity for blood plasma is 73%, and blood serum is 78.8% at wavelength 1.6 µm. But we have optimized our PCF in wavelength of 1.33 µm and we get 66.7% relative sensitivity for blood plasma and 70.02% relative sensitivity for blood serum.

Blood serum and Blood plasma relative sensitivity comparison with increase and decrease of core sector diameter D has been shown in Figs. 4 and 5, respectively. From Figs. 4, 5, we may conclude that the change of relative sensitivity is slightly higher/lower with the change of sector diameter D. A zoom version of the small portion of the curve of both Figs. 4 and 5 has been shown. From both curves, we may illustrate that if we increase + 5 µm of the sector diameter D, then the relative sensitivity will increase a small amount. Still, it will cause a problem due to fabrication as in the term of air filling ratio.

The amount of light that penetrates through cladding region is called confinement loss. Microstructure optical fiber has leaky behavior which indicates confinement loss. Confinement loss depends on geometrical properties and limiting frequency of the photonic crystal fiber. The larger the core area the larger amount of light passes through micro-structured optical fiber. Confinement loss for blood serum and plasma has been shown in Fig. 6. The figure shows that blood plasma shows lower confinement loss than Blood serum, although both blood serum and plasma show ultralow confinement loss. For both of the components confinement loss curve exhibits similar types

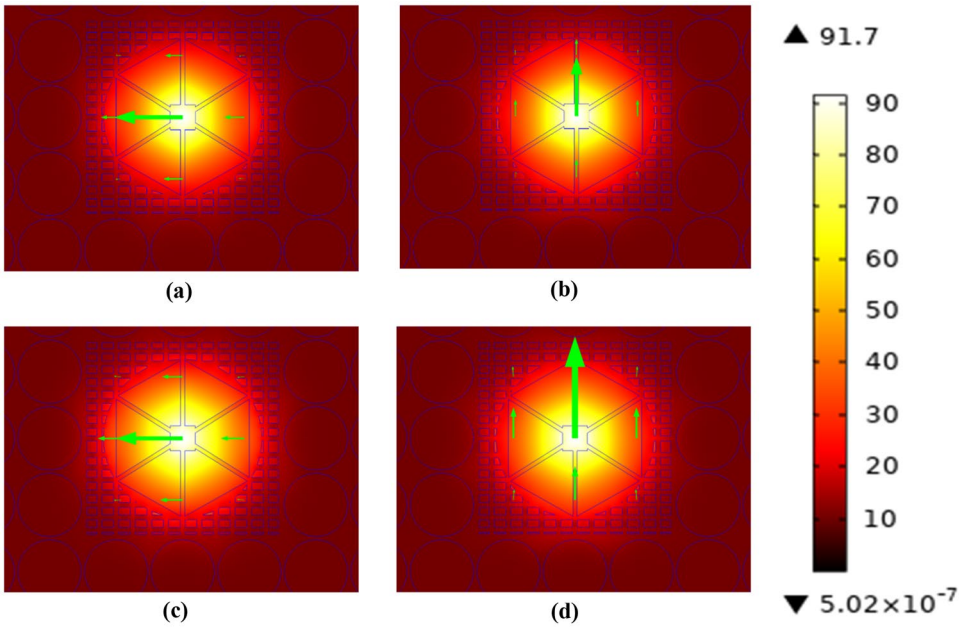

Fig. 2 Thermal view of power distribution of fundamental modes of **a** Blood plasma x-Axis **b** Blood plasma y-axis **c** Blood serum x-axis **d** Blood serum y-axis

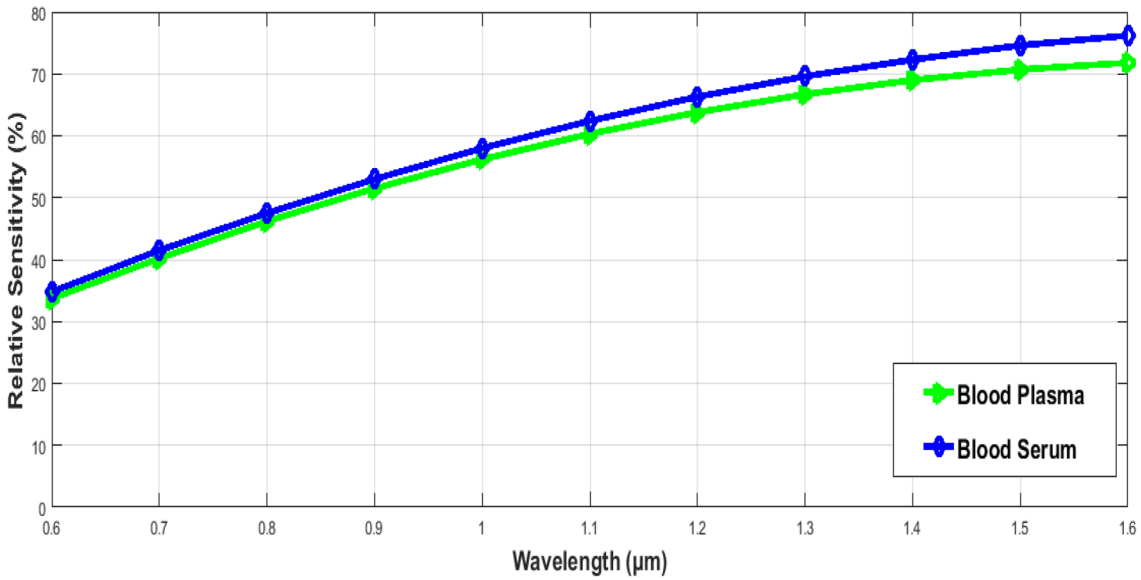

Fig. 3 Relative sensitivity for blood plasma and blood serum vs wavelength

of behavior. The confinement loss curve decreases quickly with wavelength up to 1.2 μm, and then up to 1.6 μm, the curve is almost flat. Lowest confinement loss has been gained at 1.6 μm. For blood plasma lowest confinement loss has been achieved 10^{-12} (dB/m) approximately and for blood serum the lowest confinement loss has been achieved 10^{-11} (dB/m) approximately at wavelength 1.6 μm. In this research we have investigated the proposed PCF with blood serum and plasma at a wavelength from 0.6 to 1.6 μm. At this operating frequency light interacts at core region tightly.

The difference between polarization along the x-axis and the y-axis is called birefringence, shown in Fig. 7. Birefringence is an important factor for photonic crystal fiber based sensor. Birefringence property can be achieved by asymmetrical structure of proposed photonic crystal fiber. According to the intrinsically high index contrast micro-structured optical fiber or photonic crystal fiber shows better birefringence property than other conventional optical fiber. From the figure is can be depicted that Birefringence is higher. This Birefringence curve in the figure is constant with respect to the wavelength. Furthermore, Birefringence increases linearly

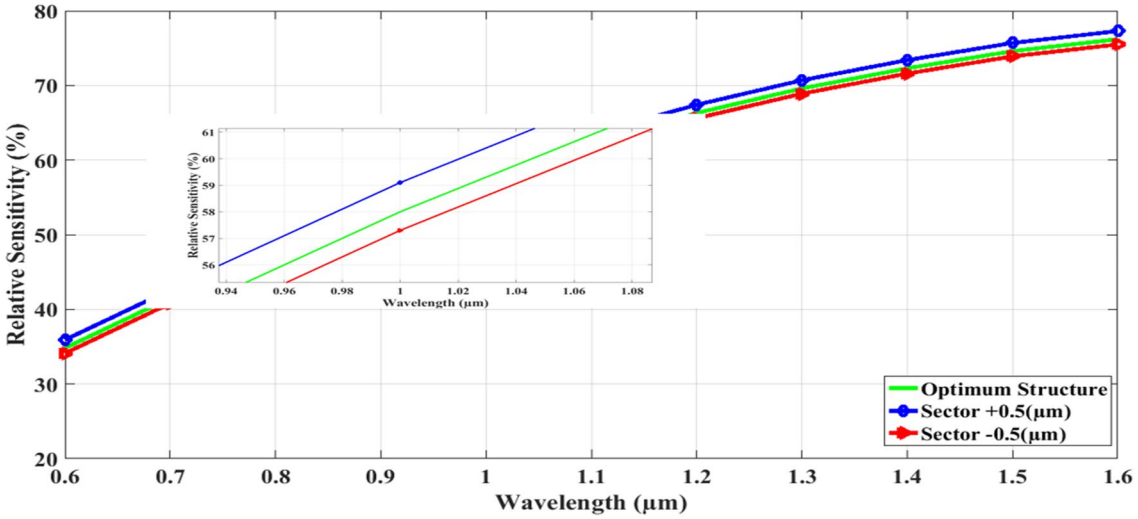

Fig. 4 Relative sensitivity vs wavelength for blood serum at different sector diameter (D)

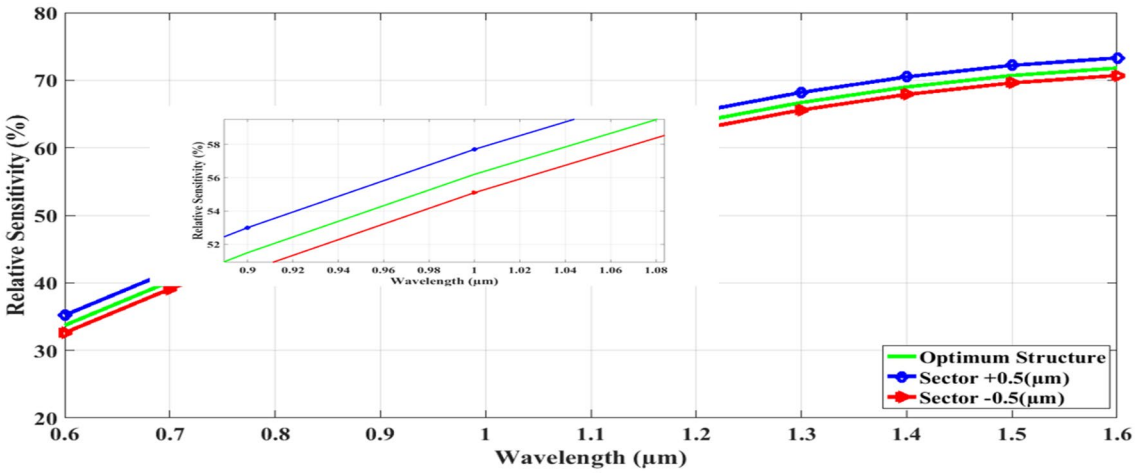

Fig. 5 Relative sensitivity vs wavelength for blood plasma at different sector diameter (D)

after 0.8 μm wavelength. For blood plasma and blood serum both cases birefringence are not same (slight deviation) from 0.6 to 1 μm. from 1.1 to 1.6 μm the both blood plasma and blood serum curve almost same.

Interaction area between light matter and proposed fiber is called effective area. Figures 8 and 9 illustrate the Effective area (*A*eff) and nonlinearity (γ) for Blood Serum and Blood Plasma, respectively. From Eqs. 7 and 8, it can be depicted that the relation between Effective Area and Nonlinearity is inversely proportional. In Fig. 8 the effective area and nonlinearity curve has been shown for blood serum. The figure depicts that the curve of the effective area and nonlinearity curve are flat from 0.6 μm to 1 μm both. At the wavelength 1.33 μm we get Effective area (Aeff) of 6.1 μm^2 and Nonlinearity (γ) of 18.68 (W^{-1} km^{-1}). On the other hand in Fig. 8 the effective area and nonlinearity curve has been shown for blood plasma. The figure depicts that the curve of the effective area and nonlinearity curve are flat from 0.6 μm to 1 μm both. At the wavelength 1.33 μm we get Effective area (A_{eff}) of 6.01 μm^2 and Nonlinearity (γ) of 20.08 (W^{-1} km^{-1}). We have taken wavelength 1.33 μm to optimize the proposed PCF. So from both figures, we can describe that the increase of effective area with wavelength decreases nonlinearity.

Although the length of the proposed PCF will be small, we have to calculate the effective material loss. In microstructured optical fiber, different background materials have been used. Absorbance by background material of

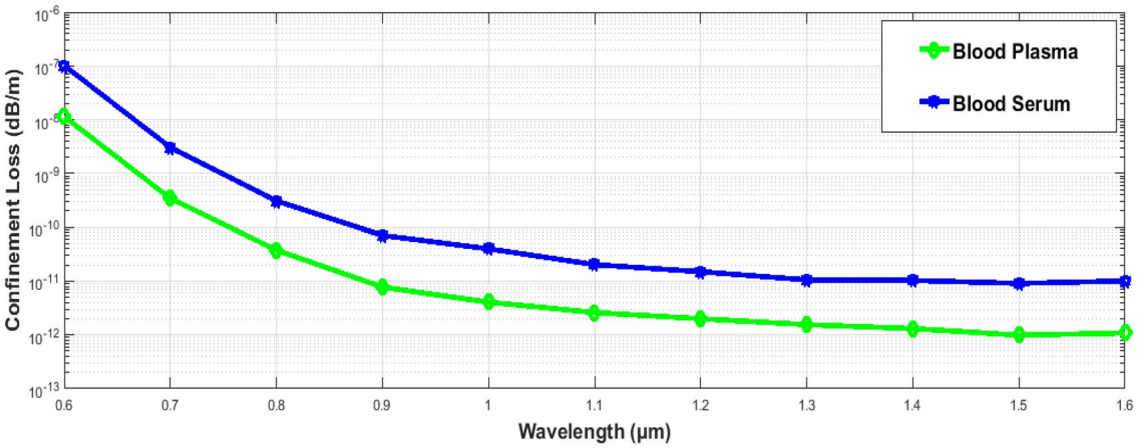

Fig. 6 Confinement loss vs wavelength for blood plasma and blood serum

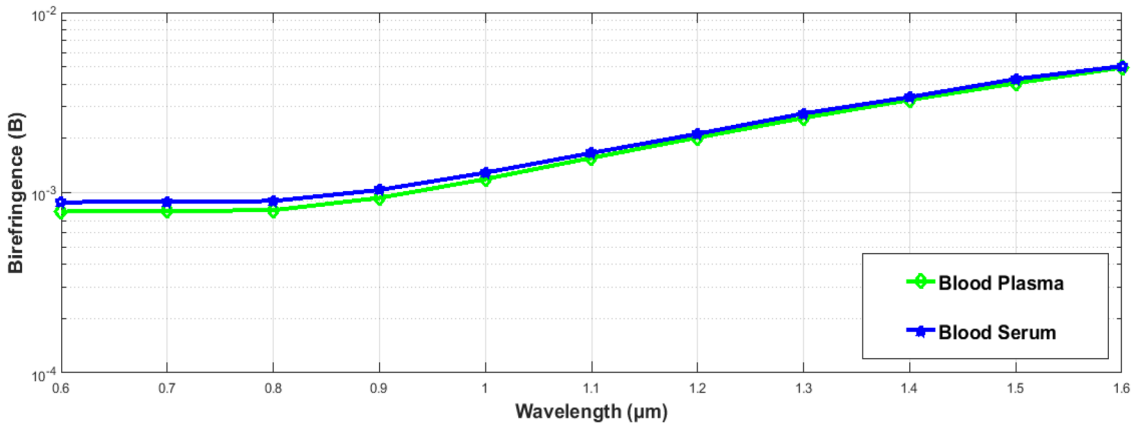

Fig. 7 birefringence vs. the wavelength for blood plasma and Serum

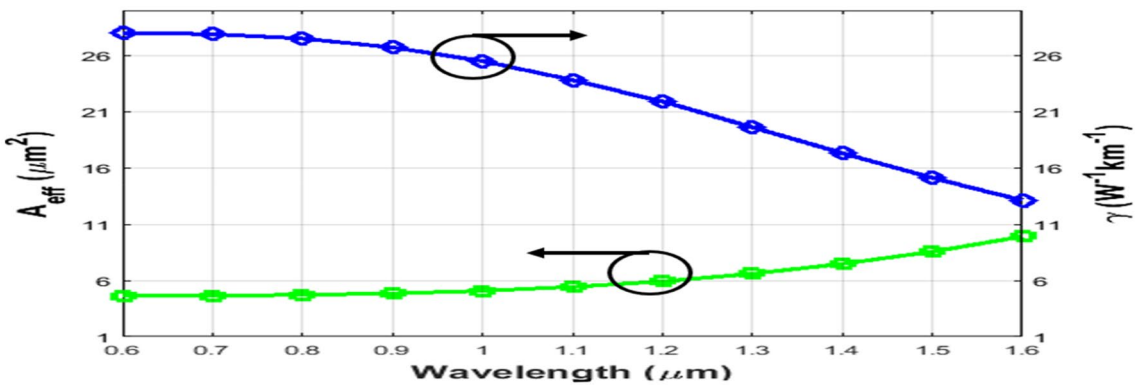

Fig. 8 Effective area (A_{eff}) and nonlinearity (γ) vs wavelength for blood serum

photonic crystal fiber causes effective material loss. The proposed PCF shows lower EML, which has been demonstrated in Fig. 10. The EML increases at a small rate with respect to wavelength up to 1.2 μm and 1.3 μm, but after that, it decreases. At wavelength 0.5 μm lowest EML has been achieved for blood serum 0.14 (cm^{-1}) and for blood plasma 0.139 (cm^{-1}). Higher EML can be found at 1.3 μm for blood serum 0.219 (cm^{-1}) and for blood plasma 0.217

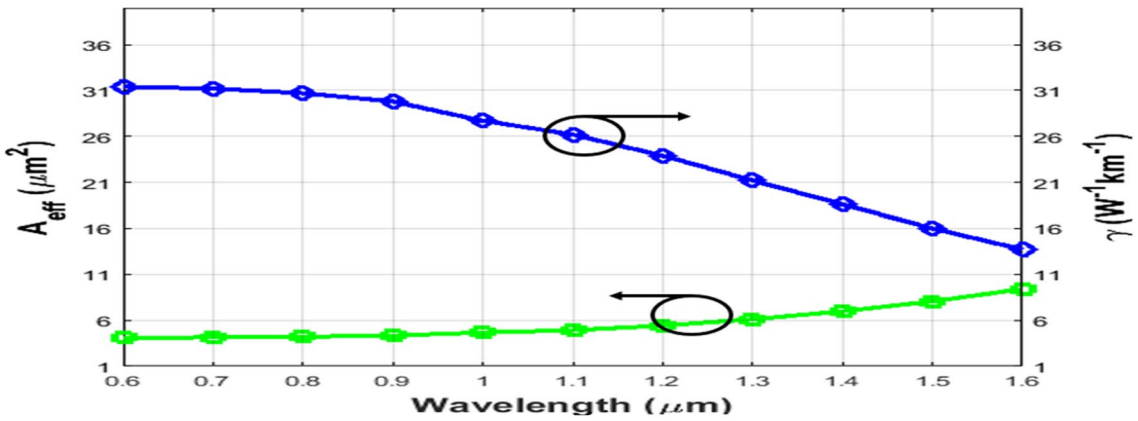

Fig. 9 Effective area (A_{eff}) and nonlinearity (γ) Vs wavelength for blood plasma

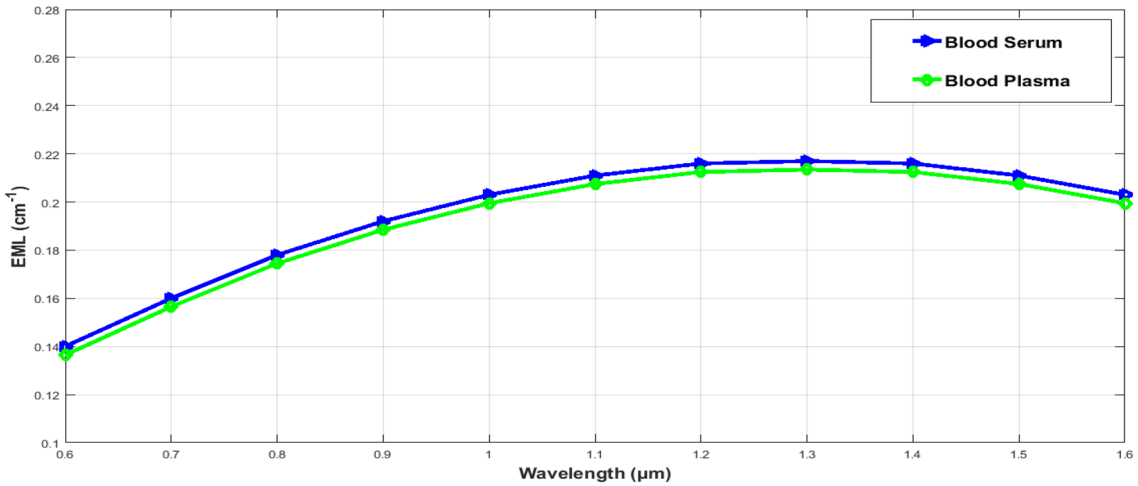

Fig. 10 EML vs wavelength for blood serum and plasma

(cm^{-1}). The electromagnetic wave goes with higher intensity and succinctly confined in the core which abridges the probability of light material interaction for a hollow core PCF structure, accordingly, EML is brought down at more eminent frequency.

The light compiled ability of any photonic crystal fiber is called Numerical Aperture which is a quantitative scale as well. Wider range of NA is expected for micro-structured optical fiber. Numerical Aperture has been shown in Fig. 11, which must be high. Our HS-SPCF shows high NA in Fig. 11. From the figure, serum shows lower NA than blood plasma, where both of the blood components NA decrease with wavelength change. At wavelength 0.6 μm NA has been achieved for blood plasma is 0.357 and for blood serum is 0.339 which is higher. On the other hand lower NA has been gained in for blood plasma is 0.242 and for blood serum is 0.239 at the wavelength 1.6 μm. To optimize the proposed PCF structure we have taken NA for blood plasma 0.286 and for blood serum 0.281 at the wavelength of 1.33 μm.

Figure 12 shows the convergence error for the proposed HS-PCF as the photonic crystal fiber has been designed at COMSOL multiphysics. The figure shows that the convergence error is very low for the proposed PCF sensor. Furthermore, the error decreases with the higher iteration number. In [25] authors proposed a PCF which is a Ring Resonator based Photonic Crystal Fiber for blood components like RBC, WBC, blood plasma sensing. transmission Spectrum has been shown as sensing mechanism.

Table 2 states the comparison between the previously proposed HS-SPCF and the proposed HS-SPCF. Here we have compared sensing of Blood Plasma at a certain wavelength of 1.33 μm. From the table, it is clear that the proposed PCF depicts higher sensitivity for plasma than the previous PCFs. Besides, the proposed PCF also shows the ultralow confinement loss /leakage loss than the prior PCFs. For the

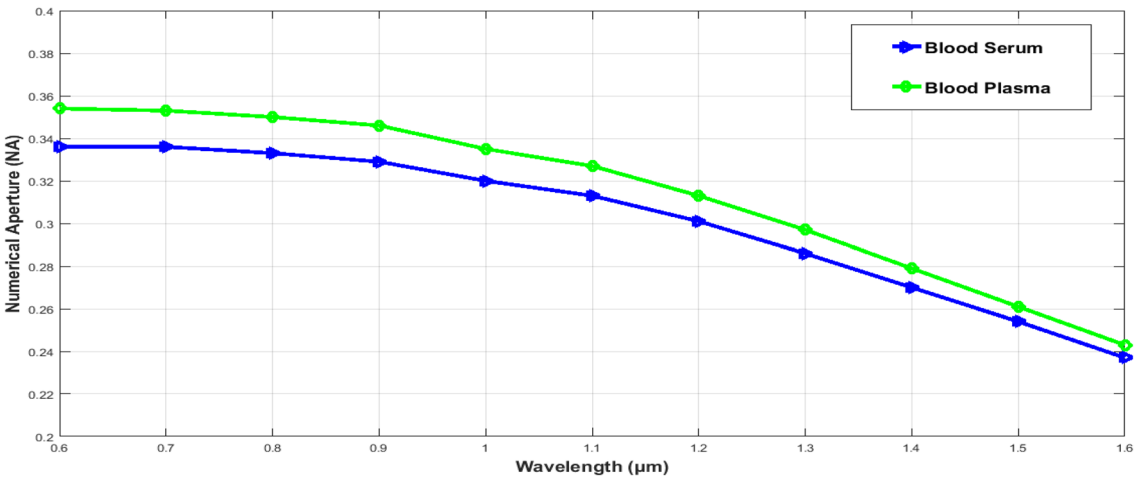

Fig. 11 Numerical aperture vs. the wavelength for blood serum and plasma

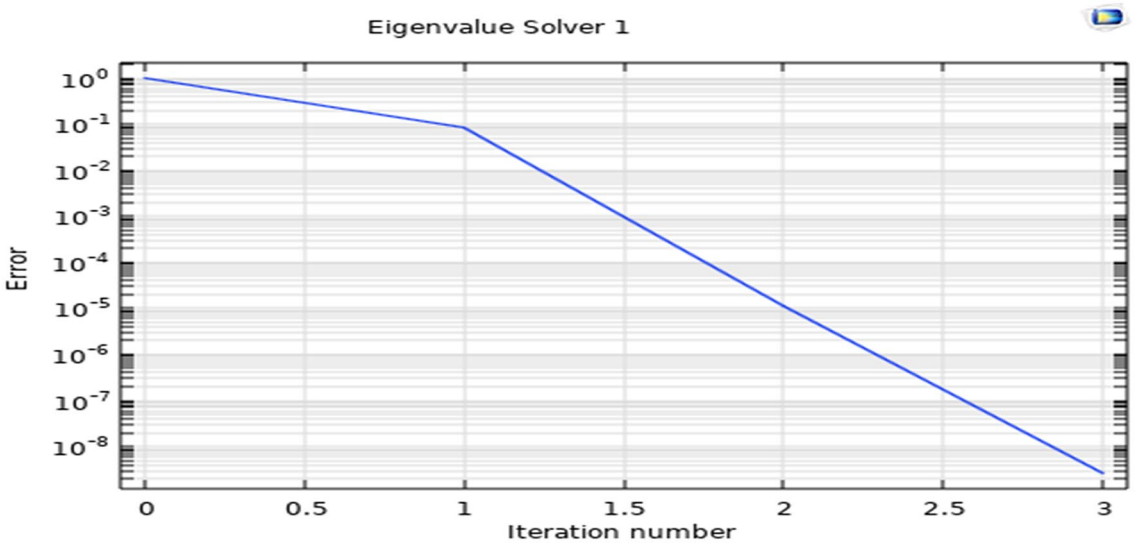

Fig. 12 Error vs iteration no of the convergence error

Table 2 Comparative analysis of the previous and proposed PCF for blood plasma at wavelength 1.33 μm

Refs.	Relative sensitivity (%)	Confinement loss	Birefringence	EML (cm^{-1})	NA	A_{eff} (μm^2)	PCF structure
[26]	55	10^{-4}	–	–	–	–	Ring core circular cladding (C-PCF)
[27]	58	10^{-5}	–	–	–	–	Ring core circular cladding (SC-PCF)
Proposed PCF	66.7	1.55×10^{-12}	2.6×10^{-3}	0.21247	0.286	6.1	Hexa-sectored cored –hybrid square cladding

proposed PCF, other optical characteristics, birefringence, effective material loss, numerical aperture, effective area, has also been investigated. The structure is less complex than the prior PCFs for fabrication. Fabrication and designing is a significant and challenging phase for photonic crystal fiber. Our proposed Photonic crystal fiber contains a hybrid square cladding with circular and square holes, but it is now possible to fabricate these types of PCF. Center Hexa-sectored core region is also simple for fabrication with the advanced fabrication techniques [28–30]. The practical consequence

of the paper is that our suggested structure clarifies better results in terms of sensitivity birefringence, confinement loss, EML, NA, effective area at the same time as the previous structure. The proposed structure can be a potential candidate for sensing Blood plasma and serum faster rate with low cost.

Blood Components like serum or plasma sensing is a very important issue in recent times. The proper ratio of blood components presents in the blood is very important. As a result, we need blood component sensing. There are conventional blood component sensors presented in [31, 32]. But there are a large number of limitations and sensing errors of the conventional sensors. Photonic Crystal Fibers sense the liquids like blood components with a higher effective rate. PCF based sensors can be used as a low-cost sensors. As a result, many researchers use PCFs for blood components sensing [33].

The main motivation of the research is to design and numerically investigate a novel PCF based liquid (blood components) sensor. We have designed and numerically investigated a PCF that shows higher relative sensitivity means that the proposed HS-PCF can sense the blood components than previous sensors. There are few limitations like designing and fabrication of the PCF as it is a nanostructure. But recent advances of the fabrication techniques like sol–gel, capillary staking, chemical vapor deposition techniques [34, 35], our proposed PCF can be designed and fabricated easily using those methods. Complex structures can be fabricated by three steps- preparation, polishing and coating [36]. Our proposed PCF is structured with two types of geometrical formation at core. Capillary Stacking methods can be used here. Sol–gel techniques can be used to fabricate cladding region. Blood serum and plasma can be filled using chemical vapor deposition techniques.

4 Conclusion

A square cladding hexa-sectored core-based PCF has been proposed in this research, which shows higher relative sensitivity for blood plasma and blood serum sensing. The hexa-sectored core region contains the analytes (blood serum / blood plasma), which interacts with light and shows sensitivity. The proposed sensor shows ultralow confinement loss and higher birefringence. Besides, effective material loss, numerical aperture, effective area (A_{eff}), and nonlinearity (γ) are some of the significant optical properties, which have also been investigated numerically using the finite element method. The Refractive index of blood (Serum/Plasma) and background material silica has been mathematically achieved by Cauchy's equation and Sellmeier equation, respectively. The operating wavelength range was kept long in investigating optical properties, which shows a high working range of the suggested PCF. The suggested HS-SPCF can be used for other blood components as well as biosensing applications.

Acknowledgements This study was funded by the Deanship of Scientific Research, Taif University Researchers Supporting Project number (TURSP-2020/08), Taif University, Taif, Saudi Arabia.

Declarations

Conflict of interest All the authors approved for submission as well as no competing interests.

References

1. J.C. Knight, T.A. Birks, P. St, J. Russell, D.M. Atkin, All-silica single-mode optical fiber with photonic crystal cladding. Opt. Lett. **21**(19), 1547–1549 (1996)
2. J.C. Knight, P. St, J. Russell, New ways to guide light. Science **296**(5566), 276–277 (2002)
3. T.-W. Lu, P.-T. Lee, Ultra-high sensitivity optical stress sensor based on double-layered photonic crystal microcavity. Opt. Express **17**(3), 1518–1526 (2009)
4. Y.-H. Chang, Y.-Y. Jhu, Wu. Chien-Jang, Temperature dependence of defect mode in a defective photonic crystal. Opt. Commun. **285**(6), 1501–1504 (2012)
5. W.-C. Lai, S. Chakravarty, Yi. Zou, R.T. Chen, Multiplexed detection of xylene and trichloroethylene in water by photonic crystal absorption spectroscopy. Opt. Lett. **38**(19), 3799–3802 (2013)
6. E.K. Akowuah, T. Gorman, H. Ademgil, S. Haxha, G.K. Robinson, J.V. Oliver, Numerical analysis of a photonic crystal fiber for biosensing applications. IEEE J. Quantum Electron. **48**(11), 1403–1410 (2012)
7. P. Hu, X. Dong, W.C. Wong, L.H. Chen, K. Ni, C.C. Chan, Photonic crystal fiber interferometric pH sensor based on polyvinyl alcohol/polyacrylic acid hydrogel coating. Appl. Opt. **54**(10), 2647–2652 (2015)
8. C.-Y. Li, B.-B. Song, Wu. Ji-xuan, W. Huang, Wu. Xu-jie, C. Jin, Dual-demodulation large-scope high-sensitivity refractive index sensor based on twin-core PCF. Optoelectron. Lett. **17**(4), 193–198 (2021)
9. S. Asaduzzaman, K. Ahmed, B. K. Paul, Slotted-core photonic crystal fiber in gas-sensing application. In *Advanced Sensor Systems and Applications VII*, vol 10025 (International Society for Optics and Photonics, 2016), p. 100250O
10. Md.S. Islam, B.K. Paul, K. Ahmed, S. Asaduzzaman, Rhombic core photonic crystal fiber for sensing applications: modeling and analysis. Optik **157**, 1357–1365 (2018)
11. Md.I. Islam, M. Khatun, S. Sen, K. Ahmed, S. Asaduzzaman. Spiral photonic crystal fiber for gas sensing application. In *2016 9th International Conference on Electrical and Computer Engineering (ICECE)*, pp. 238–242. IEEE (2016)
12. B.K. Paul, Md.S. Islam, K. Ahmed, S. Asaduzzaman, Alcohol sensing over O+ E+ S+ C+ L+ U transmission band based on porous cored octagonal photonic crystal fiber. Photonic Sensors **7**(2), 123–130 (2017)
13. C. Zhang, Q.W. Song, C.Y. Ku, R.B. Gross, R.R. Birge, Determination of the refractive index of a bacteriorhodopsin film. Opt. Lett. **19**(18), 1409–1411 (1994)
14. A. Brunsting, P.F. Mullaney, Differential light scattering from spherical mammalian cells. Biophys. J. **14**(6), 439–453 (1974)

15. C.G. Rylander, O.F. Stumpp, T.E. Milner, N.J. Kemp, J.M. Mendenhall, K.R. Diller, A.J. Welch, Dehydration mechanism of optical clearing in tissue. J. Biomed. Opt. **11**(4), 041117 (2006)
16. J.N. Adkins, S.M. Varnum, K.J. Auberry, R.J. Moore, N.H. Angell, R.D. Smith, D.L. Springer, J.G. Pounds, Toward a human blood serum proteome: analysis by multidimensional separation coupled with mass spectrometry. Mol. Cell. Proteomics **1**(12), 947–955 (2002)
17. H. Li, L. Lin, S. Xie. Refractive index of human whole blood with different types in the visible and near-infrared ranges. In *Laser-Tissue Interaction XI: Photochemical, Photothermal, and Photomechanical*, vol 3914. (International Society for Optics and Photonics, 2000), pp. 517–521
18. O.S. Zhernovaya, V.V. Tuchin, I.V. Meglinski, Monitoring of blood proteins glycation by refractive index and spectral measurements. Laser Phys. Lett. **5**(6), 460 (2008)
19. M.I. Islam, K. Ahmed, S. Sen, B.K. Paul, M.S. Islam, S. Chowdhury, A.N. Bahar, Proposed square lattice photonic crystal fiber for extremely high nonlinearity, birefringence and ultra-high negative dispersion compensation. J. Opt. Commun. **40**(4), 401–410 (2019)
20. S. Asaduzzaman, K. Ahmed, Proposal of a gas sensor with high sensitivity, birefringence and nonlinearity for air pollution monitoring. Sens. Bio-Sens. Res. **10**, 20–26 (2016)
21. S. Liu, Z. Deng, J. Li, J. Wang, N. Huang, R. Cui, Q. Zhang et al., Measurement of the refractive index of whole blood and its components for a continuous spectral region. J Biomed. Opt. **24**(3), 035003 (2019)
22. H. Ding, J.Q. Lu, W.A. Wooden, P.J. Kragel, Hu. Xin-Hua, Refractive indices of human skin tissues at eight wavelengths and estimated dispersion relations between 300 and 1600 nm. Phys. Med. Biol. **51**(6), 1479 (2006)
23. K. Ahmed, F. Ahmed, S. Roy, B.K. Paul, M.N. Aktar, D. Vigneswaran, M.S. Islam, Refractive index-based blood components sensing in terahertz spectrum. IEEE Sens. J. **19**(9), 3368–3375 (2019)
24. M.M.A. Eid, M.A. Habib, M.S. Anower, A.N.Z. Rashed, Hollow core photonic crystal fiber (PCF)–based optical sensor for blood component detection in terahertz spectrum. Braz. J. Phys. **51**(4), 1017–1025 (2021)
25. P. Sharma, P. Sharan, Design of photonic crystal based ring resonator for detection of different blood constituents. Opt. Commun. **348**, 19–23 (2015)
26. S. Singh, V. Kaur. Photonic crystal fiber sensor based on sensing ring for different blood components: design and analysis. In *2017 Ninth International Conference on Ubiquitous and Future Networks (ICUFN)*, pp. 399–403. IEEE, 2017.
27. V. Kaur, S. Singh, Design approach of solid-core photonic crystal fiber sensor with sensing ring for blood component detection. J. Nanophotonics **13**(2), 026011 (2019)
28. H. Chen, D. Chen, Z. Hong, Squeezed lattice elliptical-hole terahertz fiber with high birefringence. Appl. Opt. **48**(20), 3943–3947 (2009)
29. S. Wang, Z. Li, Yu. Chunlei, M. Wang, S. Feng, Q. Zhou, D. Chen, Hu. Lili, Fabrication and laser behaviors of Yb3+ doped silica large mode area photonic crystal fiber prepared by sol–gel method. Opt. Mater. **35**(9), 1752–1755 (2013)
30. G. Palma-Vega, C. Hupel, J. Nold, S. Kuhn, J. Limpert, N. Haarlammert, and T. Schreiber. Simplified manufacturing of advanced microstructured fibers for laser applications. *Fiber Lasers XVIII: Technology and Systems*, vol 11665. (International Society for Optics and Photonics, 2021), p. 116651S
31. M.K. Annika, Enejder, Johannes Swartling, Prakasa Aruna, Stefan Andersson Engels, Influence of cell shape and aggregate formation on the optical properties of flowing whole blood. Appl. Opt. **42**(7), 1384–1394 (2003)
32. M. Friebel, M.C. Meinke, Determination of the complex refractive index of highly concentrated hemoglobin solutions using transmittance and reflectance measurements. J. Biomed. Opt. **10**(6), 064019 (2005)
33. S.M.B.A. Riyadh, M.M. Hossain, H.S. Mondal, M.E. Rahaman, P.K. Mondal, "Photonic crystal fibers for sensing applications. J. Biosens. Bioelectron. **9**, 251 (2012)
34. R.T. Bise, D.J. Trevor, Sol-gel derived microstructured fiber: Fabrication and characterization, in *Optical Fiber Communication Conference* (Optical Society of America, 2005), p. OWL6
35. A. Ghazanfari, W. Li, M.C. Leu, G.E. Hilmas, A novel freeform extrusion fabrication process for producing solid ceramic components with uniform layered radiation drying. Additive Manuf. **15**, 102–112 (2017)
36. Y. Wang, G. Jiang, Z. Yu, Q. Wang, X. Jiang, Trapezium-shaped groove photonic crystal fiber plasmon sensor for low refractive index detection. Sens. Bio-Sens. Res. **34**, 100452 (2021)